



# Numerical Study of Double Diffusive Convection in a Lid Driven Cavity with Linearly Salted Side Walls

N. Reddy and K. Murugesan<sup>†</sup>

*Mechanical and Industrial Engineering Department, Indian Institute of Technology Roorkee, Roorkee – 247 667, India*

<sup>†</sup>Corresponding Author Email: [krimufme@iitr.ac.in](mailto:krimufme@iitr.ac.in)

(Received February 24, 2016; accepted July 26, 2016)

## ABSTRACT

Double diffusive convection phenomenon is widely seen in process industries, where the interplay between thermal and solutal (mass) buoyancy forces play a crucial role in governing the outcome. In the current work, double diffusive convection phenomenon in a lid driven cavity model with linearly salted side walls has been studied numerically using Finite element simulations. Top and bottom walls of the cavity are assumed cold and hot respectively while other boundaries are set adiabatic to heat and mass flow. The calculations of energy and momentum transport in the cavity is done using velocity-vorticity form of Navier-Stokes equations consisting of velocity Poisson equations, vorticity transport, energy and concentration equations. Galerkin's weighted residual method has been implemented to approximate the governing equations. Simulation results are obtained for convective heat transfer for  $100 < Re < 500$ ,  $-50 < N < 50$  and  $0.1 < Ri < 3.0$ . The average Nusselt number along the hot wall of the cavity is observed to be higher for higher Richardson number when buoyancy ratio is positive and vice versa. Maximum Nusselt number is recorded at buoyancy ratio 50 and Richardson number 3.0, on the other hand low Nusselt number is witnessed for buoyancy ratio  $-50$ .

**Key words:** Double diffusive mixed convection; Mass buoyancy force; Convective heat transfer.

## NOMENCLATURE

|       |   |                   |  |
|-------|---|-------------------|--|
| C     | concentration of species                    | $\beta_c$         | concentration volumetric expansion coefficient |
| D     | binary diffusion coefficient                | $\beta_T$         | thermal volumetric expansion coefficient       |
| g     | gravitational acceleration                  | $\mu$             | dynamic viscosity                              |
| H     | height of the cavity                        | $\nu$             | kinematic viscosity                            |
| N     | buoyancy ratio                              | $\alpha$          | thermal diffusivity                            |
| Nu    | local Nusselt number                        | $\phi$            | non dimensional concentration of species       |
| Pr    | Prandtl number                              | $\Theta$          | non-dimensional temperature                    |
| Re    | Reynolds number                             | $\rho$            | density  |
| Ri    | Richardson number                           | $\tau$            | non dimensional time                           |
| Sc    | Schmidt number                              | $\omega$          | vorticity                                      |
| Sh    | local Sherwood number                       | $\Omega$          | non dimensional vorticity                      |
| t     | time  | $\Delta$          | difference                                     |
| T     | temperature                                 |                   |  |
| u, v  | horizontal and vertical velocity components |                   |  |
| U, V  | non-dimensional velocity components         | <b>Subscripts</b> |  |
| $U_0$ | lid velocity                                | av                | average  |
| x, y  | horizontal and vertical coordinates         | c                 | cold   |
| X, Y  | non dimensional coordinates                 | h                 | hot  |

## 1. INTRODUCTION

Double diffusive mixed convection flows find wide engineering applications in the field of chemical

engineering processes like chemical vapour deposition, food processing, nuclear reactors and nuclear waste disposal facilities, in natural phenomenon like oceanography, solar ponds and

other applications like solar distillation, solidification processes, cooling towers, lubricating groves, cooling of electronic devices etc. (Alleborn *et al.* (1999); Ma and Walker (2000); Charaborty and Dutta (2003); Achoubir *et al.* (2008); Raham *et al.* (2012)) In such flows the nature of solutal buoyancy forces plays a key role on heat and fluid convection in the system and these can be classified as natural convection type when inertial forces are insignificant and mixed convection type otherwise. Over the years research has been conducted on double diffusive convection in simple cavity models to analyse the various effects corresponding to aiding and opposing interactions of thermo-solutal buoyancy forces under different operating conditions and fluid systems. An initial investigation on double diffusive natural convection in a simple cavity filled with moist air conducted by Costa (1997) explored the dependency of temperature and concentration fields on buoyancy ratio. They showed that solutal buoyancy effect can very well control the natural convection in a device designed only for a good thermal insulation. A double diffusive study in a rectangular cavity with horizontal counteracting temperature and concentration gradients has been studied by Lee and Hyun (1997). Their main emphasis was on the study of evolution of thermal and concentration fields for low, medium and high range buoyancy ratios. The observation showed an interesting multi-layered flow structure established in the interior core for moderate range of buoyancy ratios. Qin *et al.* (2014) extended the above work and explored the flow structure under similar circumstances. They found that flow structure is stable and understandable for fluids with larger Prandtl number but for those with less than unity the flow is found to be unstable and bifurcation of vortices are observed. Such vortex formation and bifurcations are more clearly presented by Chen *et al.* (2013) from their transient simulation study in a three dimensional geometry with horizontal thermal and concentration gradients. Teamah *et al.* (2011) has carried out numerical investigations in a square cavity with segmental heat sources for a wide range of governing non-dimensional parameters. They reported that increase in Rayleigh number, Prandtl number, non-dimensional heater length enhances heat transfer rate.

Few extended the research to cavities with different aspect ratios and examined the role of buoyancy ratio under aiding and opposing flows. Wee *et al.* (1989) has chosen a rectangular cavity of aspect ratio seven in both horizontal and vertical positions. The model had proved good for a wide range of cases especially in the region of low temperature and moisture gradients. Chena *et al.* (2010) carried out numerical investigations on the effect of buoyancy ratio, aspect ratio on flow field in a vertical annulus under opposing thermal and concentration gradients. They observed one large vortex at buoyancy ratio less than unity whereas number of vortices has varied with change in aspect ratio at buoyancy ratio greater than unity. Trevisan and Bejan (1987) studied combined temperature and concentration buoyancy effects in a rectangular slot with uniform heat and mass fluxes along the

vertical sides analytically. Nazari *et al.* (2005) investigated double diffusive natural convection in a cavity with hot obstacle for different Lewis and Rayleigh numbers. They observed number of multi cell circulations with increases in Rayleigh number and Lewis numbers but such cells disappeared with increase in buoyancy ratio. Corcine *et al.* (2015) from his study on double diffusive natural convection in a cavity observed increasing trend in heat transfer rate with increase in both Rayleigh number and Prandtl number. They came up with correlations for Nusselt number and Sherwood number for this differentially heated cavity problem.

The role of inertial forces greatly manipulates the heat and mass transfer rate in thermo-solutal-buoyancy aided flows. Lid driven cavities are one such example where inertial forces generated by lid moment plays crucial role on heat and mass exchange within the system. Understanding the flow pattern and significance of various non-dimensional parameters under the combined influence of inertial and thermo-solutal buoyancy forces acting at different magnitudes and directions has become an interesting question of research. Kumar *et al.* (2010) examined the thermo-solutal mixed convection inside a lid-driven cavity when thermal and solutal gradients act in the vertical direction. These investigations revealed that the presence of inertial forces in such system enhances the heat and mass transfer only when the thermo-solute forces are of the same magnitude or even higher than the fluid inertial forces. Another important observation from this work is that aiding solutal buoyancy forces could enhance heat transfer only at Richardson number greater than unity. Amiri *et al.* (2007) contributed further on understanding the role of different parameters in a similar kind of lid-driven cavity with vertically acting thermal and solutal buoyancy forces. They observed higher heat transfer rates at low Richardson number and higher mass transfer rates at higher Lewis number. Hasanuzzam *et al.* (2012) found that the effect of Lewis number is insignificant on flow and thermal fields at low Richardson number in his study on a triangular solar collector model. This argument is well supported by Abdalla *et al.* (2007) in his study on lid-driven cavity problem. An important observation in this work is that slowing down of main vortex by vortex break down is a cause for reduction in heat and mass transfer rate and such phenomenon is observed more at negative buoyancy ratios. Effect of buoyancy ratio is further investigated in detail by Mahapatra *et al.* (2013) in their system with both horizontal and vertical buoyancy forces generated by heating and salting of one of the horizontal and vertical walls. They found that thermal boundary layer becomes thinner with increase in buoyancy ratio which leads to conduction dominant heat transfer. Few researcher conducted numerical experiments on double diffusive convection in porous media (Gaikwad and Kamble 2014, 2016; Ayachi *et al.* (2010)) while few other focused on MHD double diffusive convection (Maatki *et al.* (2016); Chand *et al.* (2011); Bhadauria and Kiran (2015)). Kumar *et al.* (2011) had attempted a lid-driven cavity problem with a heated

block located inside the cavity. They explored the influence of the block at different aspect ratios on net heat and mass exchange of the system under various operating parameters like buoyancy ratio, and Richardson number when buoyancy forces were assumed to act in both aiding and opposing modes. Bhadauria and Kiran (2015); Kumar *et al.* (2011) conducted stability analysis on double diffusive stationary convection in a coupled stress fluid. Rani *et al.* (2013) studied double diffusive convection in flow past vertical cylinder with the same couple stress fluid.

All the above works focussed mainly on flow situation where the solutal buoyancy force acts in line with the thermal buoyancy forces like both thermal and concentration sources are set on the same walls or on opposite walls giving rise to inline opposing or aiding flows. However, in many real life engineering applications, the thermal and solutal boundary conditions are not simple. In this work one such problem has been considered, where the rate of heat transfer from hot horizontal wall to the fluid in a cavity has been investigated in the presence of mass transport from varying strength concentration source on side walls. The role of mass contamination from side walls on the thermal convection has been analysed in detail for different operating conditions. The effects of buoyancy ratio, Richardson number and Reynolds number on convective heat transfer inside the cavity are presented with the help of various contours and plots. Results for flow field, temperature, concentration and Nusselt number have been discussed in detail in for the range of parameters,  $100 < Re < 300$ ,  $0.1 < Ri < 3$ ,  $-50 < N < 50$ .

## 2. GOVERNING EQUATIONS

Flow is assumed incompressible and Boussinesq approximation is introduced for density variation due to thermal and solutal buoyancy forces. The governing equations in velocity-vorticity form are represented as follows:

Vorticity transport equation:

$$\frac{\partial \omega}{\partial t} + (\mathbf{V} \cdot \nabla) \omega = \nu \nabla^2 \omega + \nabla \times [g \beta_T (T - T_\infty)] + \nabla \times [g \beta_c (C - C_\infty)] \quad (1)$$

where  $\omega$  is the vorticity component,  $\mathbf{V} = (u, v)$  are the velocity components in x- and y-directions, respectively,  $T$  is temperature,  $C$  is concentration,  $\alpha$  is thermal diffusivity,  $D$  is mass transfer diffusion coefficient, and the subscript  $\infty$  refers to a reference state.

Velocity Poisson equation:

$$\nabla^2 \mathbf{V} = -\nabla \times \omega \quad (2)$$

Energy equation:

$$\frac{\partial T}{\partial t} + \mathbf{V} \cdot (\nabla T) = \alpha \nabla^2 T \quad (3)$$

Solutal concentration equation:

$$\frac{\partial C}{\partial t} + \mathbf{V} \cdot (\nabla C) = D \nabla^2 C \quad (4)$$

Equations (1), (2), (3) and (4) are the dimensional form of governing equations for double-diffusive mixed convection in velocity-vorticity form. These equations can be made non-dimensional by using the following scaling parameters: spatial coordinates,  $X = x/H$ ,  $Y = y/H$ , velocities,  $U = u/U_0$ ,  $V = v/U_0$ , vorticity,  $\Omega = \omega H/U_0$ , time,  $\tau = U_0 t/H$ , temperature,  $\Theta = T - T_c/T_h - T_c$ , and solutal concentration,  $= C - C_c/C_h - C_c$ .

The non-dimensional numbers are defined as, the buoyancy ratio  $N = \beta_c \Delta C / \beta_T \Delta T = GR_c / GR_T$ , Richardson number,  $Ri = GR_T / Re^2$ , Prandtl number,  $Pr = \nu / \alpha$ , Schmidt number,  $Sc = \nu / D$ , and Reynolds number,  $Re = U_0 H / \nu$ , in which  $U_0$  is the reference velocity and cold wall condition is assumed to be the reference state. After substituting the above scaling parameters and the non-dimensional numbers, the final governing equations in non-dimensional form can be written as

Vorticity transport equation:

$$\frac{\partial \Omega}{\partial \tau} + U \frac{\partial \Omega}{\partial X} + V \frac{\partial \Omega}{\partial Y} = \frac{1}{Re} \left( \frac{\partial^2 \Omega}{\partial X^2} + \frac{\partial^2 \Omega}{\partial Y^2} \right) + Ri \left( N \frac{\partial \phi}{\partial X} + \frac{\partial \theta}{\partial X} \right) \quad (5)$$

Velocity Poisson equations

$$\frac{\partial^2 U}{\partial X^2} + \frac{\partial^2 U}{\partial Y^2} = -\frac{\partial \Omega}{\partial Y} \quad (6a) \text{ and } (6b)$$

$$\frac{\partial^2 V}{\partial X^2} + \frac{\partial^2 V}{\partial Y^2} = \frac{\partial \Omega}{\partial X}$$

Energy equation

$$\frac{\partial \theta}{\partial \tau} + U \frac{\partial \theta}{\partial X} + V \frac{\partial \theta}{\partial Y} = \frac{1}{Re Pr} \left( \frac{\partial^2 \theta}{\partial X^2} + \frac{\partial^2 \theta}{\partial Y^2} \right) \quad (7)$$

Solutal concentration equation

$$\frac{\partial \phi}{\partial \tau} + U \frac{\partial \phi}{\partial X} + V \frac{\partial \phi}{\partial Y} = \frac{1}{Re Sc} \left( \frac{\partial^2 \phi}{\partial X^2} + \frac{\partial^2 \phi}{\partial Y^2} \right) \quad (8)$$

Equations (5-8) are the final equations that have to be solved for the variables  $U, V, \Omega, \Theta$  with the above boundary conditions. The boundary conditions for vorticity are determined using second order accurate Taylor's series expansion scheme. The governing equations are solved using Galerkin's weighted residual finite-element method by implementing the global matrix-free finite element algorithm.

## 3. SOLUTION METHODOLOGY

The governing equations for vorticity, velocity, energy, concentration corresponding to flow field, temperature and solutal concentration fields are

solved using Galerkin’s weighted residual finite element method with appropriate initial and boundary conditions. The solution domain is first discretized into a number of bilinear Isoparametric elements and for each element the partial differential governing questions are approximated using discretization techniques. Second order-accurate Crank–Nicolson scheme is used for discretization of time derivatives. The solution for field variable like vorticity, velocity, solutal concentration, temperature is assumed to be converged for time step ‘n+1’ when the error between two successive iterations ‘i’ and ‘i+1’ for any field variable ‘ $\eta$ ’ satisfies the following relation.

$$\sum_j^{nnode} \left( \frac{|\eta_{j+1}^i| + |\eta_j^i|}{nnode} \right) \leq 10^{-5}$$

Once the solution in all the flow fields is converged at the present time level, the iteration procedure is repeated to solve for the next time level. The algebraic equations obtained at each node are solved without assembling using global matrix free algorithm. Conjugate gradient iterative solver is employed for the solution of the final nodal equations.

#### 4. RESULTS AND DISCUSSION

##### 4.1 Problem Description

Numerical investigations have been conducted to analyse double-diffusive mixed convection in a lid-driven cavity shown in Fig. 1. Top and bottom walls are subjected to cold and hot dirichlet boundary conditions respectively whereas adiabatic conditions have been assumed for mass transfer. On the left and right vertical walls, linearly varying concentration boundaries have been assumed with adiabatic condition for heat transfer. Numerical simulations are conducted to study the effect of buoyancy ratio, Reynolds number and Richardson number on flow patterns and heat transfer within the cavity. Initial and boundary conditions used for the simulation are as follows.

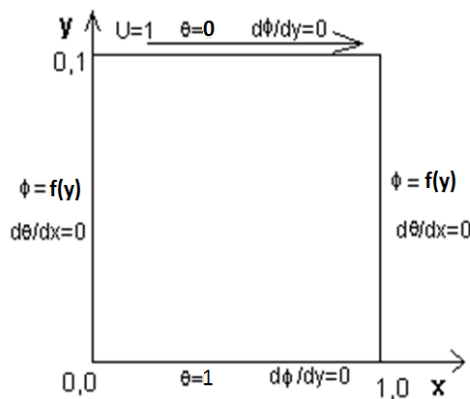


Fig. 1. Schematic diagram.

Initial and Boundary conditions:

The initial conditions are: At  $\tau = 0$  the field variables for entire domain are  $u = v = \Omega = \theta = \phi = 0$

The boundary conditions for  $\tau > 0$  are summarized as follows:

top wall:

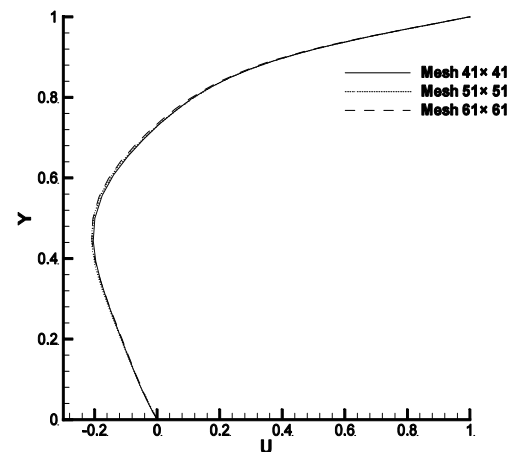
$$U = 1, V = 0, \theta = 0, \frac{\partial \phi}{\partial Y} = 0, \Omega = \nabla \times V \quad (9a)$$

bottom wall:

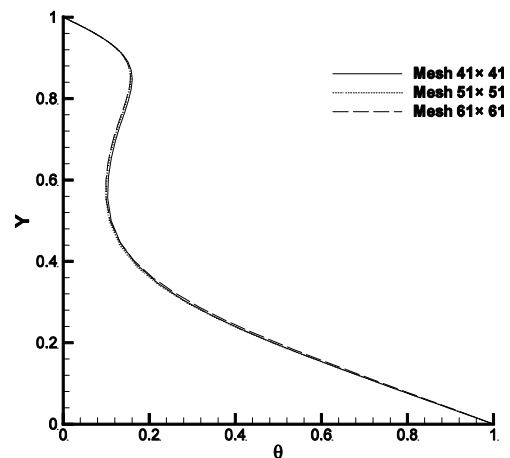
$$U = V = 0, \theta = 1, \frac{\partial \phi}{\partial Y} = 0, \Omega = \nabla \times V \quad (9b)$$

side walls:

$$U = V = 0, \phi = 1 - Y, \frac{\partial \theta}{\partial X} = 0, \Omega = \nabla \times V \quad (9c)$$



(a)



(b)

Fig. 2. Mesh sensitivity study (a) velocity plot and (b) Temperature plot at X=0.5 along Y direction.

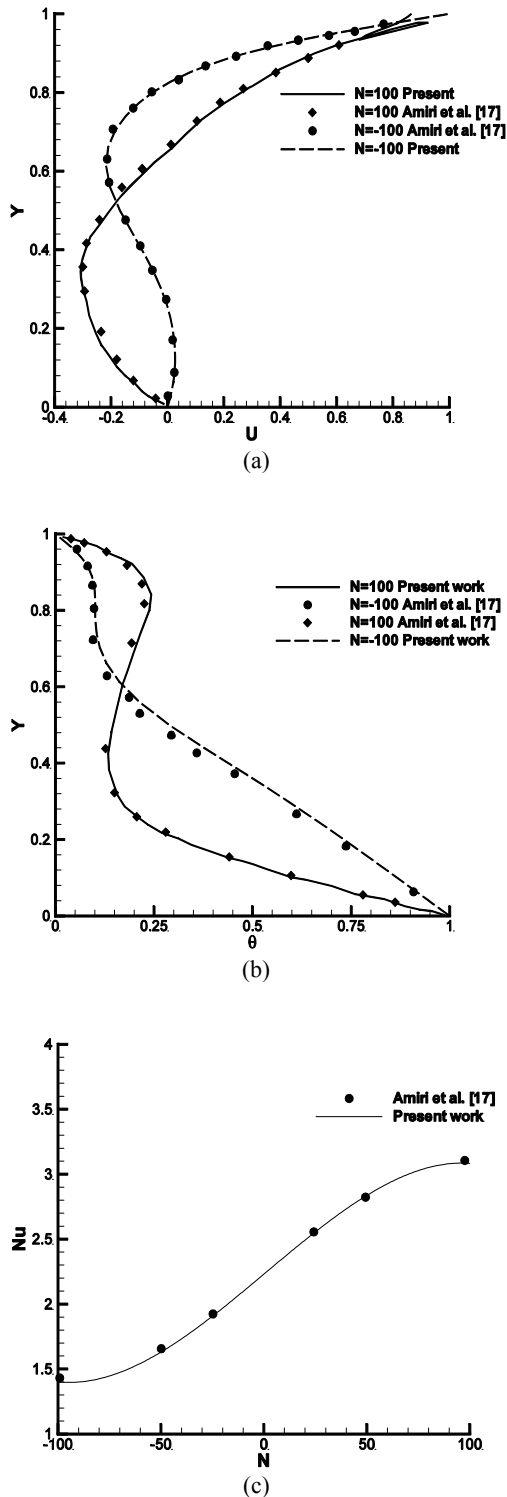


Fig. 3. Validation results: (a) Velocity (b) Temperature (c) Average Nusselt number.

#### 4.2 Mesh Sensitivity Study and Validation Results

A mesh sensitivity study has been carried out to make sure the final computational results are independent of spatial discretization of the computational domain. For this purpose the lid-driven cavity shown in Fig. 1 itself is considered.

Mesh sensitivity study has been carried out for three grids of size  $41 \times 41$ ,  $51 \times 51$  and  $61 \times 61$ . 2 shows the comparison of mid-plane distribution of temperature and U-velocity results obtained using the above three meshes for  $Re=100$ ,  $Ri=0.01$  and  $N=0$ . It can be observed from the above figures that the results obtained by all the three meshes agree very close to each other. Hence further numerical results have been obtained using the  $51 \times 51$  mesh.

The finite element code developed for the present investigation has been validated with the results reported by Al-Amiri *et al.* (2007) for a lid-driven cavity with hot temperature and high concentration on the bottom wall and cold temperature and low concentration on the top wall Dirichlet boundary conditions. Comparison of results for  $V-y$ ,  $U-y$  and  $N-Nu$  variations at  $Re=100$ ,  $Ri=0.01$ ,  $Le=1$  for  $N=-100$  to  $100$  are shown in Fig. 3(a)-(c) respectively. The results obtained using the present method is in close agreement with the results reported by Al-Amiri *et al.* (2007).

#### 4.3 Results and Discussion

The double diffusive convection in a lid-driven square cavity (Fig. 1) in the presence of linearly salted side walls is investigated. Results obtained are explained in sequence describing the effect of buoyancy ratio, Reynolds number and Richardson number followed by Nusselt number comparisons for all the cases considered.

##### 4.3.1 Effect of Buoyancy Ratio

In double diffusive convection problems, buoyancy ratio decides the relative strength of solutal and thermal buoyancy forces; for positive buoyancy ratio with increase in concentration, the density decreases and vice-versa, however, in the case of temperature variation, the density of fluid always falls down when temperature is raised. Fig. 4 gives the comparison of stream line, iso-therms, iso-concentration for different buoyancy ratio. The  $Re$  and  $Ri$  values are fixed at 100 and 1.0 respectively. Different kinds of flow structures are observed at different values of buoyancy ratio parameter ' $N$ '. At  $N=1$  when solutal and thermal buoyancy forces are of equal magnitude, the momentum from lid is carried through a large fluid vortex and a small secondary counter clock wise circulation cell at right bottom corner. With increase in buoyancy ratio  $N$  equal to 3 the primary vortex broke up early resulting in a larger secondary vortex, same phenomenon continued with further increase in buoyancy ratio. Here mass buoyancy forces are thus playing the role of minimising the main vortex and promoting the secondary circulations.

From isotherms and iso-concentration lines it is observed that iso-therms and iso-concentration lines turned steeper with increase in buoyancy ratio from 1 to 50 which gives an indication of higher heat and mass transport rates. In the current problem boundary conditions are symmetric about mid plane. Here mid plane is considered for comparisons of temperature and velocity profiles as gives unbiased results on effect of different operating parameters.

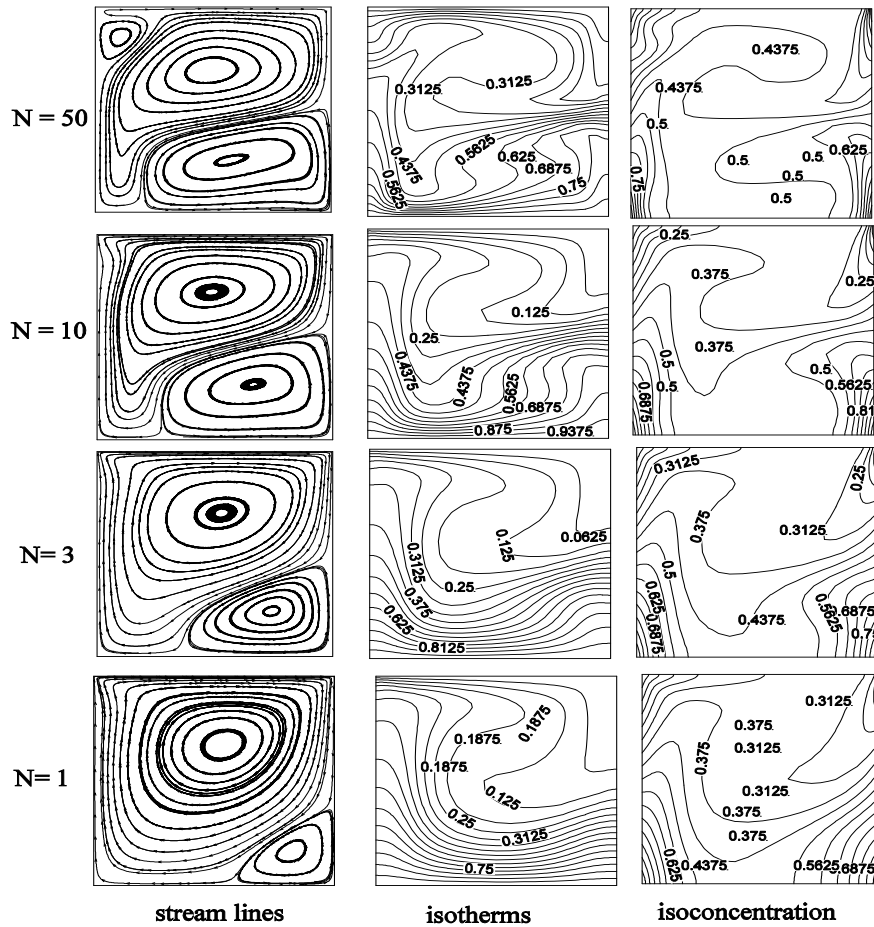


Fig. 4. Stream lines, isotherms and iso concentration lines at different buoyancy ratios in positive regime at  $Re=100$  and  $Ri=1$ .

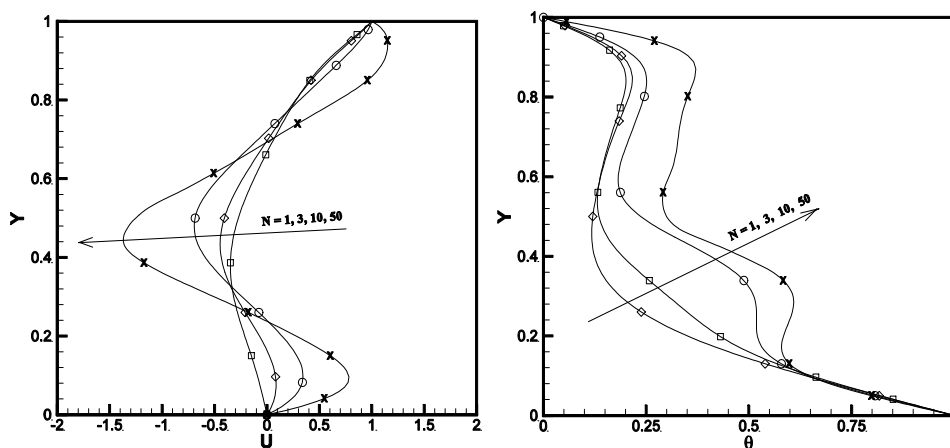


Fig. 5. Effect of buoyancy ratio on velocity (left) and temperature (right) profiles along the mid-section of the cavity for  $Ri=1$ ,  $Re=100$ .

From mid-section plots as shown in Fig. 5 it is evident that the lid velocity is transmitted more effectively deep into the cavity with increase in buoyancy ratio from 1 to 50. Temperature plots also suggest that more heat is transferred up in to the

cavity at higher buoyancy ratios. Hence in the present cavity problem the observations say that, enhancement in mass buoyancy force favours the fluid convection and heat transfer.

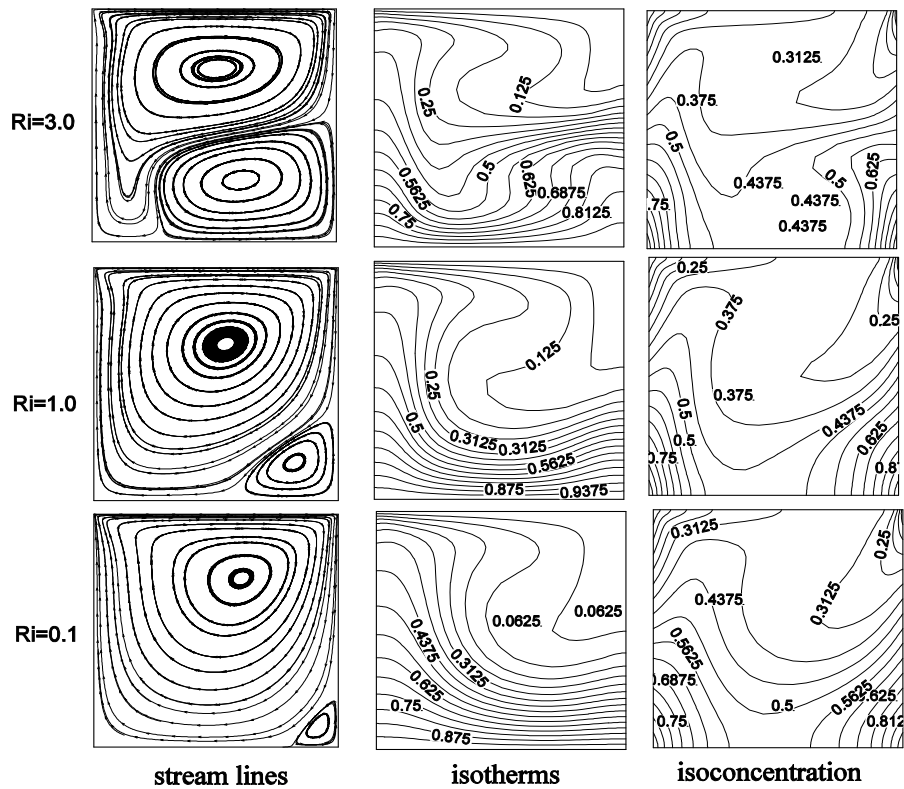


Fig. 6. Stream lines, isotherms and iso concentration lines with respect to change in Richardson number at  $N=1$  and  $Re=100$ .

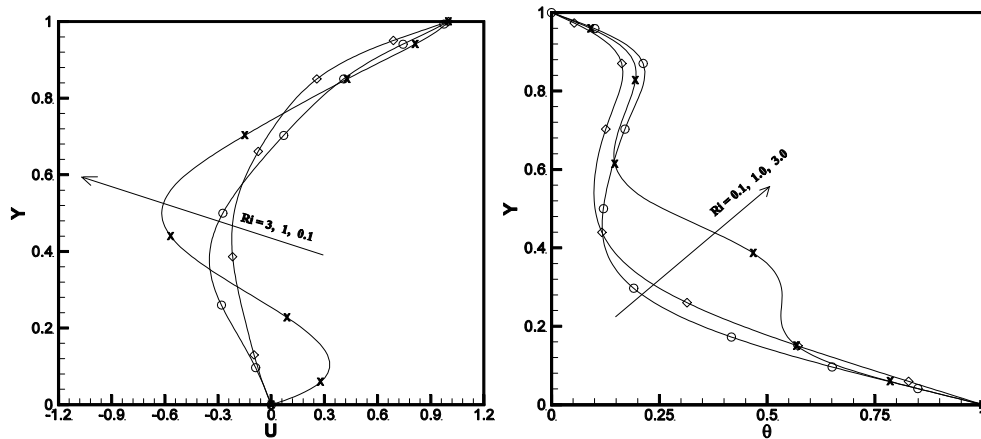
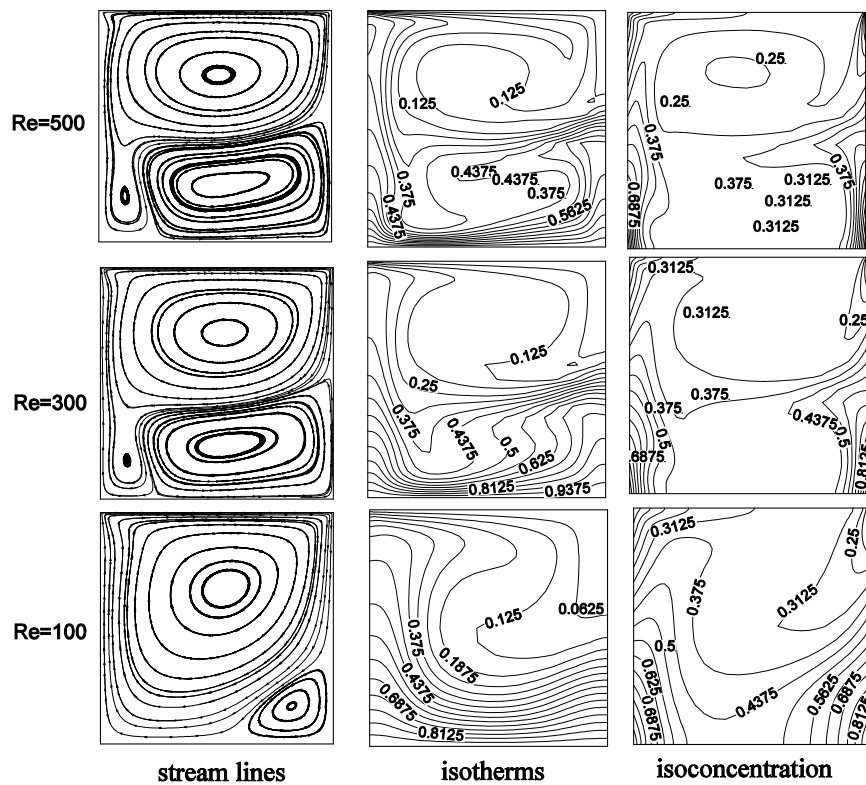


Fig. 7. Effect of Richardson number on velocity (left) and temperature (right) profiles along the mid-section of the cavity for  $N=1$ ,  $Re=100$ .

#### 4.3.2 Effect of Richardson Number

As the Richardson number increases, the role of buoyancy forces on fluid convection inside the cavity becomes stronger. Fig. 6 gives the comparison of stream line, iso-therms, iso-concentration for different Richardson number. Here the buoyancy ratio and Reynolds number were fixed at 1 and 100 respectively. At low Richardson number the effect of

buoyancy forces is low thus the inertial forces plays strong role in setting convection, thus at  $Ri=0.1$  a large primary circulating cell is observed close to lid. With increase in Richardson number the influence of thermal and mass buoyancy forces on fluid convection inside the cavity increases. In accordance to earlier discussion on effect of buoyancy ratio here too from results it is evident that size of the primary circulation cell got reduced and secondary



**Fig. 8.** Stream lines, isotherms and iso concentration lines with respect to change in Reynolds number at  $N=1$  and  $Ri=1$ .

circulations cell increased. From Fig. 6 one can notice that stream lines are observed increasingly curvier with increase in Richardson number, which tells that overall convection inside the cavity enhanced by buoyancy forces.

With increase in Richardson number Iso-concentration lines also found steeper near vertical walls indicating the effect of enhanced fluid convection inside the cavity. These results are supported by Fig. 7 where one can see that both  $U$  velocity and temperature are found dominant at higher Richardson number. Thus one can say that here with linear salting condition increase in contribution of buoyancy forces on convection is playing aiding role on overall convection and heat transfer in the cavity.

#### 4.3.3 Effect of Reynolds Number

In this section effect of increase in inertial forces on heat and momentum transport in the cavity are studied. Simulation results have been obtained for different Reynolds number i.e 100, 300 and 500 for  $N=1$ ,  $Ri=1$ . Fig. 8 illustrates the effect of  $Re$  on streamline pattern, temperature and concentration contours within the cavity.

As the Reynolds number increases the inertial forces of the fluid increases thus the fluid convection enhances. From Fig. 8 it is observed that secondary vortex grown

in size with increase in  $Re$  from 100 to 500.

This resulted in increased temperature and concentration gradients at the bottom wall and side walls respectively with change in  $Re$  from 100 to 500. Fig. 9 corresponding to mid-way plots of  $U$ -velocity and temperature along the depth of the cavity gives quantitative comparison for different Reynolds number. This plot supports the previous observation that increase in inertial forces improved the velocity from lid in to depth of the cavity and thus heat transfer from bottom wall.

From the results it is evident that solutal gradients becomes steeper with enhancement in fluid convection either by increment in  $Re$  or  $Ri$ . This enhancement in fluid convection is contributed by raise in inertial or buoyancy forces. From these observations the effect of important dimensional heat transfer parameters can be analysed accordingly. Increment in temperature range enhances strength of thermal buoyancy forces and enhancement of heat transfer coefficient 'h' or thermal conductivity 'k' increases the heat transfer rate which can strengthen the thermal convection and thus convective mass transfer. Essentially raise in temperature range contribute to raise in thermal Grashof number, Richardson number. Raise in h or k value increases the wall thermal gradients and eventually increases the strength of thermal buoyancy forces or Richardson number.

### 4.3.4 Nusselt Number

The convective heat transfer within the cavity is computed over the hot wall of the cavity, called the Nusselt number. Fig. 10 shows the variation of average Nusselt number with respect to buoyancy ratio for different Richardson number. For Positive N values at first sight one can easily understand that Nusselt number increases as buoyancy ratio increases due to positive effect of mass buoyancy on fluid convection, the reverse has happened with increase in buoyancy ratio in negative direction. It is observed that higher Richardson number contributed to higher Nusselt number when the N is positive an increased influence of buoyancy forces on fluid convection improved heat transfer. Similarly when buoyancy ratio is negative mass buoyancy forces play negative role, so here lower Richardson number contributed to higher Nusselt number as the hampering effect on fluid convection is minimized. From Fig. 10 one can observe steep decrease in Nusselt number with decrease in buoyancy ratio to -1 to -10 for Ri=1.0 and 3.0, whereas for Ri=0.1 retarding effect is gradual as the opposing buoyancy forces are less influential at low Ri. Similarly steep increase in Nusselt number is observed at Ri=3.0 in case of positive buoyancy ratio as now buoyancy forces plays supporting role.

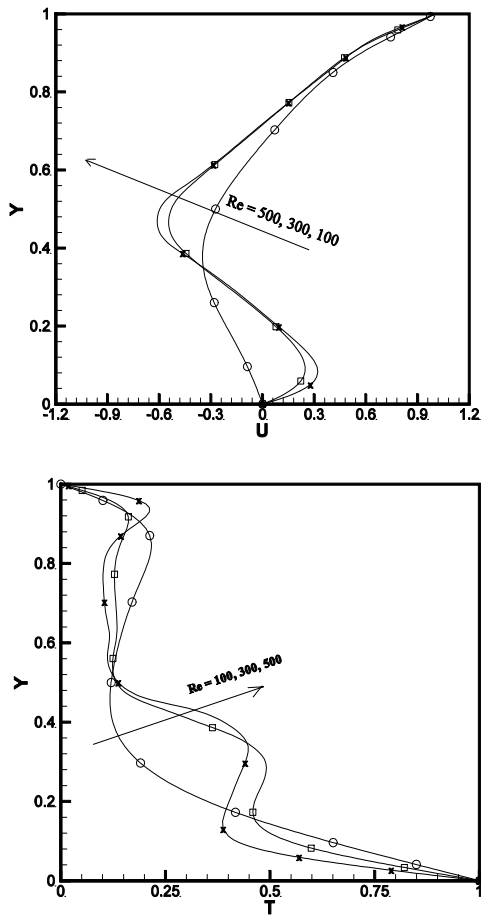


Fig. 9. Effect of Reynolds number on velocity (top) and temperature (bottom) profiles along the mid-section of the cavity for Ri=1, N=1.

Figures 11 shows the effect of Reynolds number and Richardson number on Nusselt number distributions on hot bottom wall of the cavity. Here the buoyancy ratio is chosen to be 1, which indicates that thermal and solutal buoyancy forces are of equal magnitude. The Nusselt number along hot bottom wall is found to increase with increase in Re for all the values of Richardson number, however, the rate of increase is high when operated above Re=300 due to strong inertial forces. There is a steep variation of Nu for Ri=3.0 compared to other two Richardson number, this may be due to an extra convective motion caused from buoyancy forces which are much influential at higher Ri.

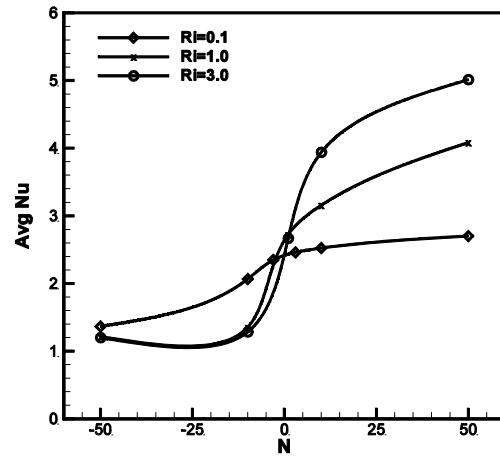


Fig. 10. Effect of Buoyancy ratio on average Nusselt number for different Richardson number at Re=100.

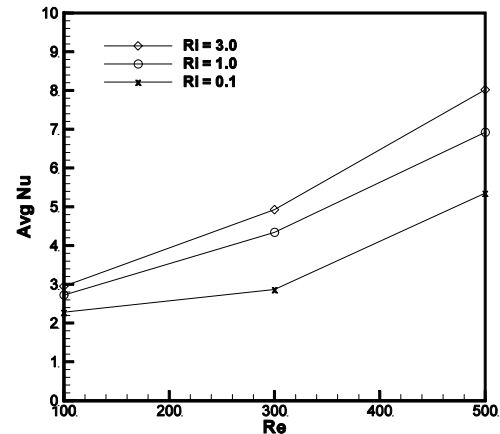


Fig. 11. Effect of Reynolds number on average Nusselt number for different Richardson numbers at N=1.

## 5. CONCLUSIONS

Numerical simulations on thermo-solutal convection in a lid-driven square cavity with salted vertical wall have been carried out. Governing equations in velocity-vorticity form are solved using a finite element based computer code. Results are presented

on effect of mass buoyancy force due to imposed linear variation in concentration on the vertical walls of the cavity on convective heat transfer under different range of operating conditions. Based on the results obtained for the analysis of the effect of buoyancy ratio, Richardson numbers and Reynolds number the following conclusions have been arrived:

- Mass buoyancy forces have showed positive effect on convective heat transfer when buoyancy ratio is positive and the reverse is observed for negative buoyancy ratios.
- Higher Richardson number favoured convective heat transfer from bottom walls when N is positive and higher Nusselt number is recorded for lower Richardson number when N is negative.
- Effect of solutal buoyancy forces are found more prominent on the rise in average Nusselt number at higher Richardson number when buoyancy ratio is positive.
- Maximum average Nusselt number of 5.01 has been recorded at  $Ri=3.0$ ,  $N=+50$  and lowest of 1.20 is recorded at  $N=-50$ ,  $Ri=3.0$  for  $Re=100$ .
- Increase in Reynolds number shown increment in average Nusselt number the rate of increase in Nusselt number is found more at higher Richardson number.

#### ACKNOWLEDGEMENTS

Our Sincere thanks to Dr. Navneet Kumar Gupta, Institute Computer Centre, Indian Institute of Technology Roorkee, for providing us the required high end computing facility to carry out the simulations.

#### REFERENCES

- Achoubir, K., R. Bennacer, A. Cheddadi, M. ElGanaoui and E. Semma (2008). Numerical study of thermosolutal convection in enclosures used for directional solidification (Bridgman Cavity). *FDMP* 4(3), 199-209.
- Al-Amiri, A. M., K. M. Khanafar and I. Pop (2007). Numerical simulation of a combined thermal and mass transport in a square lid-driven cavity. *International Journal of Thermal Science* 46, 662-671.
- Al-Amiri, A. M., K. M. Khanafar and I. Pop (2007). Simulation of a Combined Thermal and Mass Transport in a Square Lid-Driven Cavity. *International Journal of Thermal Science* 46, 662 – 671 .
- Alleborn, N., H. Rasziller and F. Durst (1999). Lid-driven cavity with heat and mass transport. *International Journal of Heat and Mass Transfer* 42, 833-853.
- Bhadauria, B. S. and P. Kiran (2015). Weak nonlinear double diffusive magneto-convection in a Newtonian liquid under gravity modulation. *Journal of Applied Fluid Mechanics* 8, (4), 735-746.
- Bhadauria, B. S., P. G. Siddheshwar, A. K. Singh and K. G. Vinod (2016). A local nonlinear stability analysis of modulated double diffusive stationary convection in a couple stress liquid. *Journal of Applied Fluid Mechanics* 9, (3), 1255-1264.
- Chakraborty, S. and P. Dutta (2003). Three-dimensional double-diffusive convection and macro segregation during non-equilibrium solidification of binary mixtures. *Int. J. Heat and Mass Transfer* 46, 2115–2134.
- Chand, P. S., A. Mahajan and P. Sharma (2011). Effect of rotation on double-diffusive convection in a Magnetized Ferrofluid with Internal Angular Momentum. *Journal of Applied Fluid Mechanics* 4 (4), 43-52.
- Chen, Z. W., J. M. Zhan, Y. S. Li, Y. Y. Luo and S. Cai (2013). Double-diffusive buoyancy convection in a square cuboid with horizontal temperature and concentration gradients. *International Journal of Heat and Mass Transfer* 60, 422-431.
- Chena, S., J. Tölke and M. Krafczyk (2010). Numerical investigation of double-diffusive (natural) convection in vertical annulus with opposing temperature and concentration. *International Journal of Heat and Fluid Flow* 31, (2), 217-226.
- Corcione, M., S. Grignaffini and A. Quintino (2015). Correlations for the double-diffusive natural convection in square enclosures induced by opposite temperature and concentration gradients. *International Journal of Heat and Mass Transfer* 81, 811-819.
- Costa, V. A. F. (1997). Double diffusive natural convection in a square enclosure with heat and mass diffusive walls. *International Journal of Heat and Mass Transfer* 40, 4061-4071.
- El Ayachi, R., A. Raji, M. Hasnaoui, A. Abdelbaki and M. Naimi (2010). Resonance of double-diffusive convection in a porous medium heated with a sinusoidal exciting temperature. *Journal of Applied Fluid Mechanics* 3(2), 43-52.
- Gaikwad, S. N. and S. S. Kamble (2014). Linear stability analysis of double diffusive convection in a horizontal sparsely packed rotating anisotropic porous layer in presence of Soret effect. *Journal of Applied Fluid Mechanics* 7(3), 459-471.
- Gaikwad, S. N. and S. S. Kamble (2016). Cross-diffusion effects on the onset of double diffusive convection in a couple stress fluid saturated rotating anisotropic porous layer. *Journal of Applied Fluid Mechanics* 9(4), 1645-1654.
- Hasanuzzaman, M., M. M. Rahman, H. F. Öztop, N. A. Rahim and R. Saidur (2012). Effect of Lewis number on heat and mass transfer in a triangular

- cavity. *International Communications in heat and mass transfer* 39, 1213-1219.
- Kumar, D. S., K. Murugesan and A. Gupta (2010). Numerical analysis of interaction between inertial and thermo-solutal buoyancy forces on convection heat transfer in a lid driven cavity. *ASME Journal of Heat transfer* 132(11).
- Kumar, D. S., K. Murugesan and H. R. Thomas (2011). Effect of the aspect ratio of a heated block on the interaction between inertial and thermosolutal buoyancy forces in a lid-driven cavity. *Numerical Heat Transfer Part A: Applications* 60, 604-628.
- Lee, J. W. and J. M. Hyun (1997). Double-diffusive convection in a rectangle with opposing horizontal temperature and concentration gradients. *International Journal of Heat and Mass Transfer* 33, 1619-1632.
- Ma, N. and J. S. Walker (2000). A parametric study of segregation effects during vertical Bridgman crystal growth with an axial magnetic field. *Journal of Crystal Growth* 208, 757-771.
- Maatki, C., W. Hassen, L. Kolsi, N. AlShammari, B. M. Naceur and H. B. Aissia (2016). 3-D numerical study of hydro magnetic double diffusive natural convection and entropy generation in cubic cavity. *Journal of Applied Fluid Mechanics* 9(4), 1915-1925.
- Mahapatra, T. R., D. Pal and S. Mondal (2013). Effects of buoyancy ratio on double-diffusive natural convection in a lid-driven cavity. *International Journal of Heat and Mass Transfer* 57, 771-785.
- Nazari, M., L. Louhghalam, M. H. Kayhani (2015). Lattice Boltzmann simulation of double diffusive natural convection in a square cavity with a hot square obstacle. *Chinese Journal of Chemical Engineering* 23, 22-30.
- Qin, Q., Z. A. Xia and Z. F. Tian (2014). High accuracy numerical investigation of double-diffusive convection in a rectangular enclosure with horizontal temperature and concentration gradients. *International Journal of Heat and Mass Transfer* 71, 405-423.
- Rahman, I. M. M., H. F. Öztop, A. Ahsan, M. A. Kalam and Y. Varol (2012). Double-diffusive natural convection in a triangular solar collector. *International Communications in Heat Mass Transfer* 39, 264-269.
- Rani, H. P. and G. J. Reddy (2013). Soret and Dufour effects on transient double diffusive free convection of couple-stress fluid past a vertical cylinder. *Journal of Applied Fluid Mechanics* 6(4), 545-554
- Teamah, M. A., M. M. K. Dawood and W. M. El-Maghlany (2011). Double diffusive natural convection in a square cavity with segmental heat sources. *European Journal of Scientific Research* 54(2), 287-301.
- Trevisan, O. V. and A. Bejan (1987). Combined heat and mass transfer by natural convection in a vertical enclosure. *Journal of Heat Transfer* 109(1), 104-112.
- Wee, H. K., R. B. Keey and M. J. Cunningham (1989). Heat and moisture transfer by natural convection in a rectangular cavity. *International Journal of Heat and Mass Transfer* 32(9), 1765-1778.